



Formation of double-side teathed nanocombs of ZnO and self-catalysis of Zn-terminated polar surface

Chang Shi Lao ^a, Pu Xian Gao ^a, Ru Sen Yang ^a, Yue Zhang ^b,
Ying Dai ^{b,c}, Zhong L. Wang ^{a,*}

^a School of Materials Science and Engineering, Georgia Institute of Technology, Atlanta, GA 30332-0245, USA

^b Department of Materials Physics, University of Science and Technology Beijing, Beijing 100083, China

^c Department of Materials Science, Wuhan University of Science and Technology, Wuhan, China

Received 3 September 2005

Abstract

Polar surface induced asymmetric growth of single-side teathed ZnO nanocombs was attributed to the self-catalysis of the Zn-terminated (0001) surface (Z.L. Wang, X.Y. Kong, J.M. Zuo, Phys. Rev. Lett. 91 (2003) 185502). In this Letter, nanocombs of ZnO with double-sided teeth have been observed. This symmetric growth of the fish-ribbon like teeth has been identified due to the existence of an inversion domain boundary along the ribbon, so that both side surfaces of the ribbon are terminated with the chemically active Zn-(0001) plane. A model is also given about the formation of $\sim 110^\circ$ double-sided nanocombs based on the nucleus composed of multiply twinned pyramids. The data show that the Zn-terminated (0001) surface is responsible for the formation of the teeth, while the oxygen-terminated (000 $\bar{1}$) surface is chemically inactive and does not grow teeth.

© 2005 Elsevier B.V. All rights reserved.

Wurtzite structured ZnO, with a wide band gap of 3.37 eV and piezoelectricity, is a good candidate for optoelectronics [1], sensors [2] and transistors [3]. Research in ZnO related nanostructures is a forefront in nanotechnology because of the diverse morphologies of nanostructures and unique properties. From crystal structure, ZnO has three types of fast growth directions: $\langle 0001 \rangle$, $\langle 01\bar{1}0 \rangle$ and $\langle 2\bar{1}\bar{1}0 \rangle$, together with the $\pm(0001)$ polar-surfaces, various unusual structural configurations have been reported, such as nanobelts [4], nanosprings [5], nanorings [6], nanohelices [7] and nanocombs [8,9].

This letter focuses on a newly found structure of ZnO: double-side teathed nanocombs. We first present the synthesis of the symmetric nanocombs. Then, its formation process will be investigated. Finally, some other types of nanocomb structures will be presented. The data clearly support that the Zn-terminated (0001) surface is chemi-

cally active for inspiring self-catalysis, which leads to the formation of the comb structure.

The synthesis of the comb-like nanostructures of ZnO is based on a high-temperature solid–vapor deposition process [4]. The experimental apparatus included a horizontal high temperature tube furnace, an enclosed alumina tube, a rotary pump, and a gas controlling system. In the experiments, 2 g of commercial (Alfa Aesa) ZnO powder was loaded on an alumina holder and placed in the center of the tube as the source material. Several pieces of polycrystalline Al_2O_3 substrates were positioned downstream as substrates to collect the products. The furnace was then heated up to 1400–1450 °C at a ramping rate of 20 °C per minute with Ar carrier gas of flowing rate of 50 sccm (standard cubic centimeters per minute) at pressure of 200–250 mbar. With a constant pressure and gas flow rate, the evaporation process was kept running for 100–150 min. Then the grown nanostructures were collected at a temperature zone of 600–800 °C. The as-synthesized structures were characterized with scanning electron microscopy

* Corresponding author. Fax: +1 404 894 9140.

E-mail address: zhong.wang@mse.gatech.edu (Z.L. Wang).

(FE-SEM, field emission LEO 1530 FEG) and transmission electron microscopy (TEM, field emission TEM Hitachi HF-2000).

Fig. 1a is a low magnification SEM image of the as-grown single-sided ZnO combs with asymmetric teeth distribution [8–12]. The yield of the nanocombs is $\sim 100\%$. A typical nanocomb is magnified and is inserted, showing many thin teeth of similar lengths and diameters growing out of a straight primary ribbon. These teeth have spacing around 200 nm, diameter ~ 50 nm and length ~ 2 μm . Fig. 1b is another configuration for the single-sided combs, in which a row of hexagonal nanowires with two segments of different diameters stacking one on the other along the length direction. From the hexagonal symmetry of the nanowire, its growth direction is $[0001]$. Fig. 1c shows a

comb structure with a series of long thin belts (40–50 μm in length, 0.5–4 μm in width), growing in parallel out of one side of the ribbon and forming a ‘waterfall-like’ configuration. In Fig. 1d, the nanocombs have a set of much wider teeth, with a wide range of inter-teeth spacing, a length from 1 to 5 μm and a width of 200–500 nm. The upper inset image reveals the quasi-rectangular shape of the cross section of the teeth. Fig. 1e is a TEM image of a typical single-sided comb structure and the corresponding electron diffraction pattern. The diffraction pattern shows that the growth direction of the teeth is $[0001]$ and of the primary ribbon is $[2\bar{1}\bar{1}0]$, and both share the same top and bottom surfaces of $\pm(01\bar{1}0)$.

The formation of one-sided asymmetric nanocombs has been attributed to the self-catalysis effect of polar surface

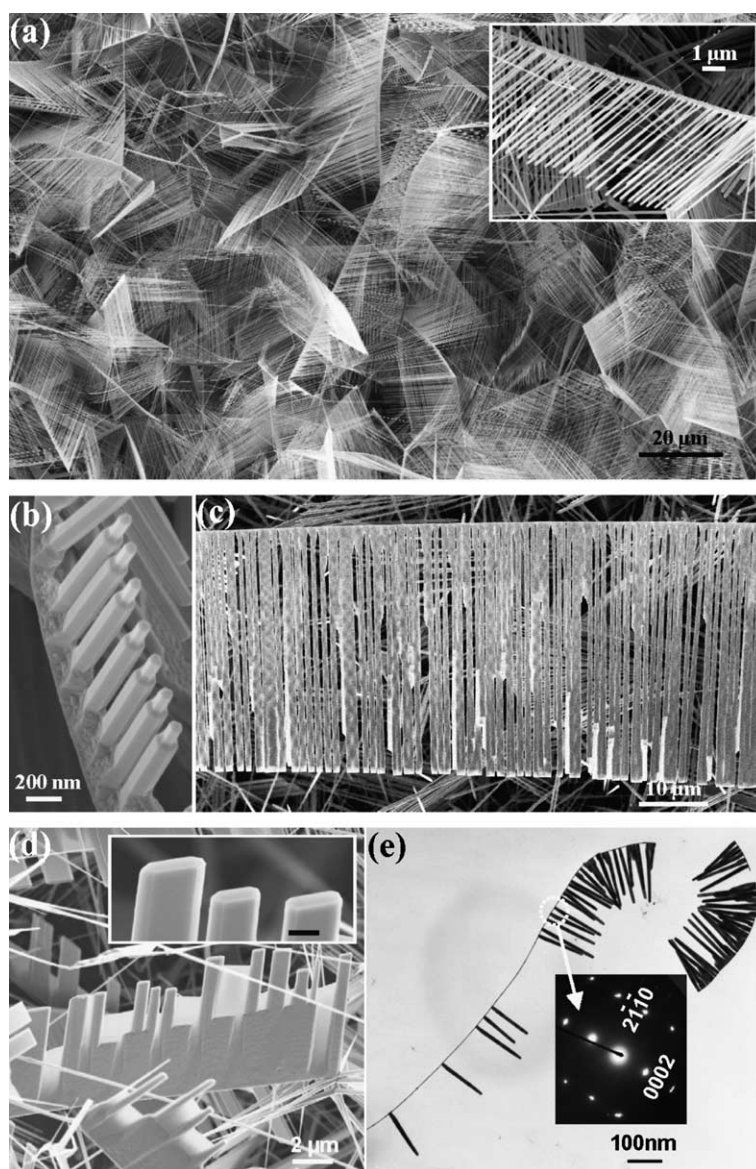


Fig. 1. (a) As-grown, single-side teathed ZnO comb structures. Inset is a magnified image of a single-sided comb; (b) to (d) are SEM images of single-sided combs with different morphologies. (e) A typical TEM image of the single-sided nanocomb. Inset diffraction pattern is from the circled area showing that the growth direction of the teeth is $[0001]$.

[9]. Due to the non-central symmetric characteristic of ZnO, the (0001) of ZnO is terminated with Zn cations, and the (000 $\bar{1}$) is terminated with oxygen anions, which are the two typical polar surfaces of ZnO, and they induce a group of unique nanostructures [13]. The Zn-(0001) surface is chemically active and its self-catalysis results in the growth of teeth on one side. The oxygen terminated (000 $\bar{1}$) surface is relatively chemically inert and produces no growth. This is the reason that the asymmetric nanocombs are most frequently received [8–12], and they can be grown almost at 100% purity.

However, symmetric nanocombs with double-sided teeth (fish-ribbon type) have also been produced in our synthesis, and sometimes the yield can be more than 80%. In Fig. 2a, a low magnification SEM image shows a high yield of the double-sided teeth comb structure. Fig. 2b is a magnified image of a symmetric comb, which clearly displays

that the teeth grow from both sides of the ribbon. Fig. 2c is another type of double-sided combs with two rows of dumbbell-like shaped teeth.

The formation of the symmetric nanocombs cannot be explained by the polar surface model if the main ribbon is a single crystal with both sides of the combs being terminated by Zn-(0001) and O-(000 $\bar{1}$), respectively. To find out the formation process of the double-sided nanocombs, we have used convergent beam electron diffraction (CBED) to determine the polarity of the two sides. Fig. 3a is a low magnification TEM image from the nanocomb, displaying a symmetric distribution of the teeth at both sides of the ribbon. The corresponding electron diffraction pattern recorded from a group of teeth is given in Fig. 3b, showing the conventional spotty pattern of [01 $\bar{1}$ 0], but there is a radial angular twist profile as indicated by the dashed lines for the {000 ℓ } series of the diffraction spots, indicating a

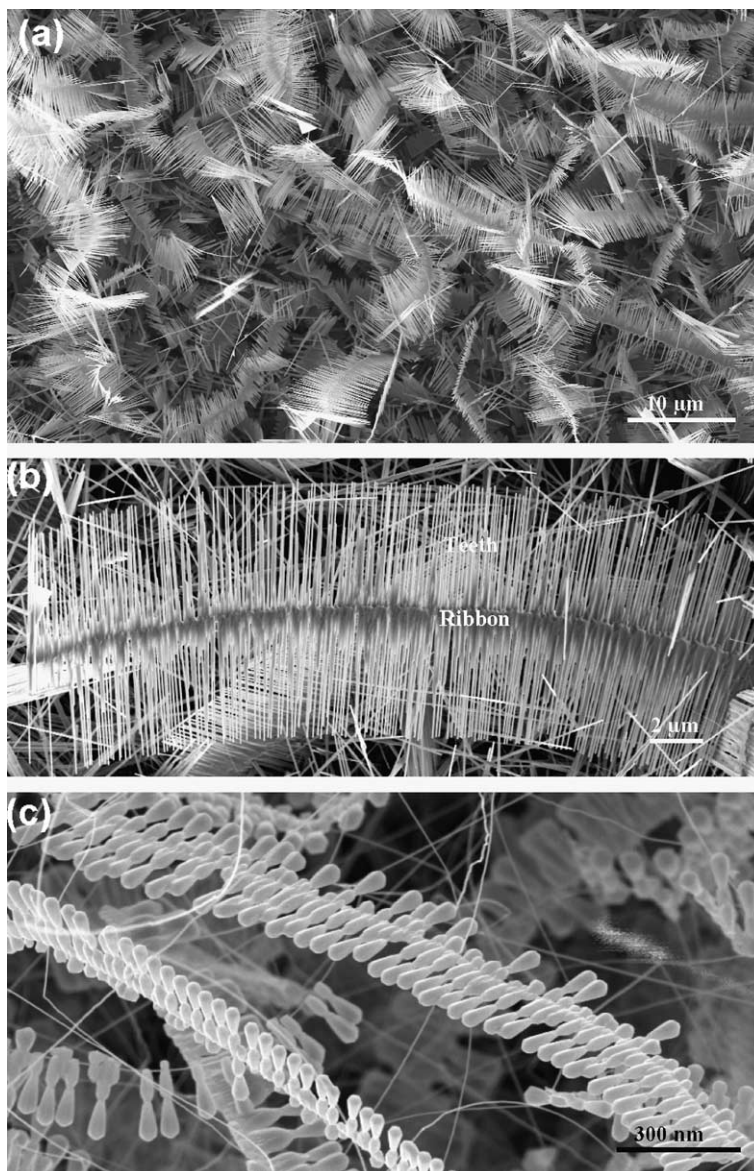


Fig. 2. SEM images of the double-side teathed ZnO comb structures. (a) A low magnification SEM image showing the high yield of the symmetric combs. (b) and (c) double-sided ZnO nanocombs with different morphologies.

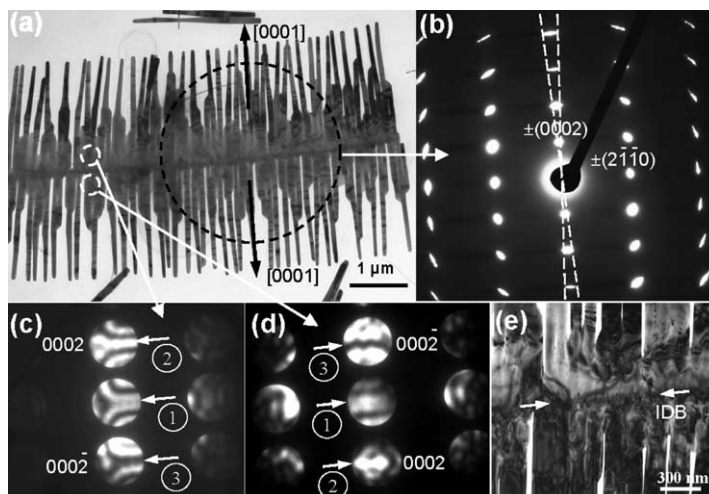


Fig. 3. (a) TEM image of a double-side teathed ZnO nanocomb. (b) Diffraction pattern from the large circled area, showing the growth direction of the teeth is $[0001]$. (c) and (d) are convergent beam electron diffraction patterns from the upper tooth and the corresponding lower tooth of the nanocomb, as indicated by the small circles. The intensity distribution in the patterns indicates that both of the teeth are along $[0001]$ direction but at 180° reversed polarity. (e) A magnified TEM image showing the existence of an inversion domain boundary parallel to the ribbon.

twist in orientation among the teeth. The comb ribbon grows along $[2\bar{1}\bar{1}0]$ (a -axis) with $\pm(01\bar{1}0)$ as the top/bottom surfaces. To determine the polarity of the nanocomb, Fig. 3c and d are the CBED patterns recorded from the two-circled areas in Fig. 3a. Caution was taken to ensure that the two CBED pattern were recorded from both sides of the ribbon at a close distance and at equivalent thickness. CBED relies on dynamic interaction of electron beam with the crystal, and it is sensitive to the symmetry of the crystal [14]. The intensity distribution in the diffraction disks can be used to identify the polarity. The intensity distributions in the (0002) and the $(000\bar{2})$ disks are significantly different, which is due to the non-central symmetric structure of ZnO. As indicated by arrowheads, the #2 disk in Fig. 3c is the mirror image of the #2 disk in Fig. 3d, the #3 disk in Fig. 3c is the mirror image of the #3 disk in Fig. 3d. Judging from the fine intensity distribution in the disks, the pattern shown in Fig. 3c is approximately 180° rotation of the pattern shown in Fig. 3d. From our previous dynamic simulations [9], the #2 disk is the (0002) diffraction disk, thus the growths of the teeth on both sides are along $[0001]$. This is only possible if there is an inversion domain boundary (IDB) parallel to the ribbon of the comb, and the structure of which was investigated in details elsewhere [15]. The IDB is a planar defect at which two ZnO crystals with inverted polarization meet at the (0001) plane following an orientation relationship of: $\mathbf{a}||\mathbf{a}'$, $\mathbf{b}||-\mathbf{b}'$ and $\mathbf{c}||-\mathbf{c}'$, where \mathbf{a} , \mathbf{b} and \mathbf{c} are the unit cell vectors for the tooth on the top part of the comb and \mathbf{a}' , \mathbf{b}' and \mathbf{c}' are those for the tooth on the lower part. An enlarged TEM image from the ribbon shows a distinct contrast line a bit off the central axis of the ribbon, as indicated by two arrowheads. With the formation of the IDB, it is possible that both sides of the ribbon are terminated with chemically active, Zn-terminated (0001) planes, resulting in the formation of the symmetrically teathed comb.

In the synthesis of the nanocomb structures, the teeth length of both single-sided and double-sided combs can be obtained from several hundred nanometers to tens of micrometers, depending on the temperature and pressure conditions for the experiments as well as the temperature zone where the substrates were placed in the furnace. In practice, nanocombs with longer teeth and the double-sided combs were acquired in a higher temperature zone.

Besides the two main comb structures reported above, other interesting comb-like structures were also found. The structure shown in Fig. 4a is the same type of asymmetric nanocomb as shown in Fig. 1, but it is directly linked to a tetraleg of ZnO [16], as indicated by an arrowhead. In Fig. 4b, the symmetric nanocomb has two-sided teeth, but the teeth are at an angle of $\sim 110^\circ$. In Fig. 4c, a feather-like comb structure is shown, which has a similar structure as the one shown in Fig. 4b except the image was taken at an angle with the ribbon of the nanocomb that the angle between the two-sided teeth is not apparently shown.

The formation of the nanocombs in Fig. 4 can be explained from the octahedral multiply twined nucleus that is responsible for the formation of the tetraleg [16], as shown in Fig. 5. The central octahedral nucleus is composed of eight tetrahedra. A tetrahedron is a unit enclosed by one $\{0001\}$ facet and three $\{11\bar{2}2\}$ pyramidal facets (Fig. 5a). Eight tetrahedra are combined together to form the octahedral nucleus, with the pyramidal faces contacting with each other, the $\pm(0001)$ planes facing out in an alternative sequence, as shown in Fig. 5b. Because the (0001) plane terminated with Zn is chemically active, while the oxygen-terminated $(000\bar{1})$ surface is relatively inactive, nanowires are preferentially grow only out of the (0001) planes, thus, forming the tetraleg structure as observed in Fig. 4a. One of the legs can be a tooth for a nanocomb. If the nucleus contains only four tetrahedral units, in a shape of a half-octahedron, there are only two Zn-termi-

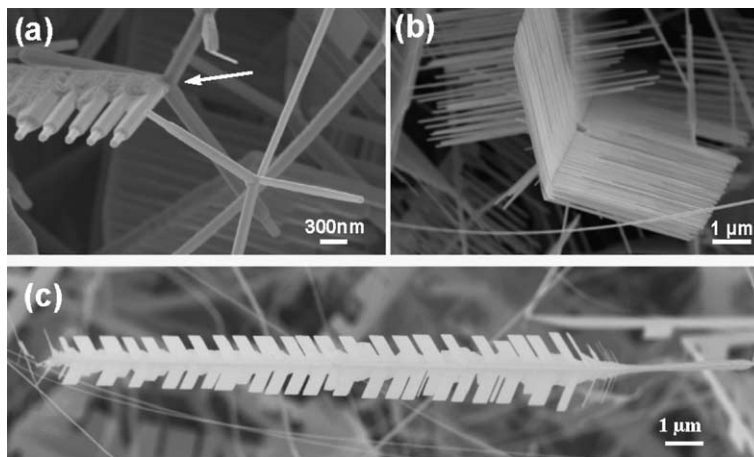


Fig. 4. (a) A single-sided nanocomb ending with a tetra-leg structure. (b) and (c) feather-like double-sided nanocombs with an angle of $\sim 110^\circ$ between the two sides.

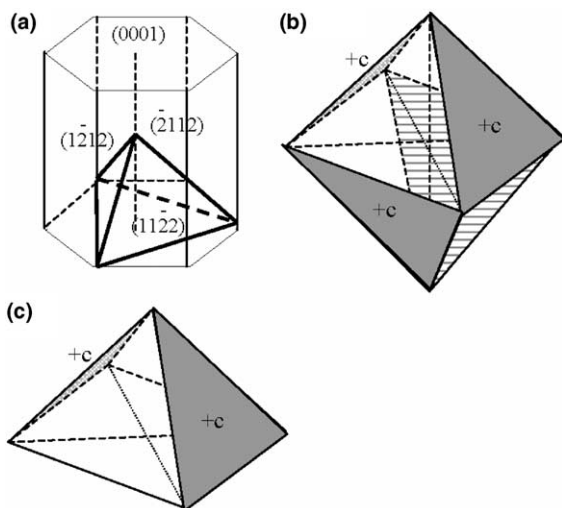


Fig. 5. The structure model about the formation of the tetraleg/tetrapole structure and the feather-like, double-sided nanocomb. (a) A pyramid crystal formed by three $\{11\bar{2}2\}$ and one (0001) facets. (b) A nucleus composed of eight twinned pyramid crystals with the $\{11\bar{2}2\}$ faces contacting with each other, the $\pm(0001)$ planes ($\pm c$) facing out in an alternative sequence. The Zn-terminated (0001) planes are shaded. (c) A half-octahedron model for the growth of the 110° angle of two-sided nanocomb.

nated (0001) planes, the growth of nanowires from the (0001) planes leads to the formation of the structures presented in Fig. 4b and c, with the teeth on both sides at an angle of $\sim 110^\circ$. Such structure was also found for ZnS [17].

In summary, single-sided and double-sided nanocomb structures were synthesized for ZnO. For the double-sided nanocombs, an inversion domain boundary is formed parallel to the $\{0001\}$ plane along the growth direction of the central ribbon, so that the two sides of the ribbon are both terminated by the Zn-terminated (0001) surfaces. The Zn- (0001) polar surface defines the growth direction of the teeth out of the ribbon. Based on the multiply twinned octahedral nucleus of ZnO, the formation of the $\sim 110^\circ$ an-

gle comb structure is also explained. Our data strongly support the active role played by the Zn-terminated (0001) plane in the growth of ZnO nanostructures.

Acknowledgments

Thanks to Jun Zhou, Jin Liu and Justin Hwa's for their help in the synthesis experiments. Thanks the support from NSF, the NASA Vehicle Systems Program and Department of Defense Research and Engineering (DDR&E), and the Defense Advanced Research Projects Agency (Award No. N66001-04-1-8903).

References

- [1] J.C. Johnson, H.Q. Yan, R.D. Schaller, L.H. Haber, R.J. Saykally, P.D. Yang, *J. Phys. Chem. B* 105 (2001) 11387.
- [2] Q. Wan, Q.H. Li, Y.J. Chen, T.H. Wang, X.L. He, J.P. Li, C.L. Lin, *Appl. Phys. Lett.* 84 (2004) 3654.
- [3] M.S. Arnold, P. Avouris, Z.W. Pan, Z.L. Wang, *J. Phys. Chem. B* 107 (2003) 659.
- [4] Z.W. Pan, Z.R. Dai, Z.L. Wang, *Science* 291 (2001) 1947.
- [5] X.Y. Kong, Z.L. Wang, *Nano Lett.* 3 (2003) 1625.
- [6] X.Y. Kong, Y. Ding, R. Yang, Z.L. Wang, *Science* 303 (2004) 1348.
- [7] P.M. Gao, Y. Ding, W.J. Mai, W.L. Hughes, C.S. Lao, Z.L. Wang, *Science* 309 (2005) 1700.
- [8] H.Q. Yan, R.R. He, J. Johnson, M. Law, R.J. Saykally, P.D. Yang, *J. Am. Chem. Soc.* 125 (2003) 4728.
- [9] Z.L. Wang, X.Y. Kong, J.M. Zuo, *Phys. Rev. Lett.* 91 (2003) 185502.
- [10] J.H. Park, H.J. Choi, Y.J. Choi, S.H. Sohn, J.G. Park, *J. Mater. Chem.* 14 (2004) 35.
- [11] Y.H. Leung, A.B. Djurisic, J. Gao, M.H. Xie, Z.F. Wei, S.J. Xu, W.K. Chan, *Chem. Phys. Lett.* 394 (2004) 452.
- [12] J.Y. Lao, J.Y. Huang, D.Z. Wang, Z.F. Ren, *J. Mater. Chem.* 14 (2004) 770.
- [13] Z.L. Wang, X.Y. Kong, Y. Ding, P.X. Gao, W.L. Hughes, R.S. Yang, Y. Zhang, *Adv. Funct. Mater.* 14 (2004) 943.
- [14] F. Vigue, P. Vennegues, S. Veizian, M. Laugt, J.-P. Faurie, *Appl. Phys. Lett.* 79 (2001) 194.
- [15] Y. Ding, X.Y. Kong, Z.L. Wang, *Phys. Rev. B* 70 (2004) 235408.
- [16] Y. Dai, Y. Zhang, Z.L. Wang, *Solid State Commun.* 126 (2003) 629.
- [17] D. Moore, C. Ronning, C. Ma, Z.L. Wang, *Chem. Phys. Lett.* 385 (2004) 8.